APL Materials

Iridium complex immobilization on covalent organic framework for effective C—H borylation

Cite as: APL Mater. **7**, 101111 (2019); https://doi.org/10.1063/1.5122674
Submitted: 30 July 2019 . Accepted: 19 September 2019 . Published Online: 14 October 2019

Harsh Vardhan, Yanxiong Pan, Zhongyu Yang, Gaurav Verma, Ayman Nafady, Abdullah M. Al-Enizi, Tawfiq M. Alotaibi, Omar A. Almaghrabi, and Shengqian Ma

Iridium complex immobilization on covalent organic framework for effective C—H borylation

Cite as: APL Mater. 7, 101111 (2019); doi: 10.1063/1.5122674
Submitted: 30 July 2019 • Accepted: 19 September 2019 •
Published Online: 14 October 2019

Harsh Vardhan,[1] Yanxiong Pan,[2] Zhongyu Yang,[2] Gaurav Verma,[1] Ayman Nafady,[3,4,a)] Abdullah M. Al-Enizi,[3] Tawfiq M. Alotaibi,[5] Omar A. Almaghrabi,[6] and Shengqian Ma[1,a)]

AFFILIATIONS

[1]Department of Chemistry, University of South Florida, 4202 East Fowler Avenue, Tampa, Florida 33620, USA
[2]Department of Chemistry and Biochemistry, North Dakota State University, 1231 Albrecht Blvd., Fargo, North Dakota 58108, USA
[3]Chemistry Department, College of Science, King Saud University, Riyadh 11451, Saudi Arabia
[4]Chemistry Department, Faculty of Science, Sohag University, Sohag 82534, Egypt
[5]King Abdullah City for Atomic and Renewable Energy, Riyadh 11451, Saudi Arabia
[6]Faculty of Science, University of Jeddah, Jeddah 21959, Saudi Arabia

Note: This paper is part of the Special Topic on Open Framework Materials for Energy Applications.
[a)]**Electronic addresses:** anafady@ksu.edu.sa and sqma@usf.edu

ABSTRACT

The strong coordination between metal ions and binding moieties in functional porous materials is central to the design and advancement of heterogeneous catalysis. In this study, we have successfully immobilized catalytically active iridium ions on a two-dimensional covalent organic framework (COF) having bipyridine moieties using a programmed synthetic procedure. The iridium immobilized framework, Ir_{cod}(I)@Py-2,2′-BPyPh COF, had high porosity, good stability, and exhibited excellent catalytic activity for C—H borylation, as compared with the pristine framework. Additionally, Ir_{cod}(I)@Py-2,2′-BPyPh COF was found to be an efficient catalyst for a series of electronically and sterically substituted substrates. The immobilized COF possessed excellent reusability, recyclability, and retention of crystallinity. This report highlights the role of porous materials as an ideal decorating platform for conducting a wide range of potent chemical conversions.

I. INTRODUCTION

Catalytic transformation of C—H bonds is extremely challenging, and an unambiguous understanding of the strategies to activate this bond is central to numerous organic transformations.[1–20] Over the past years, there has been extraordinary progress in the development of homogeneous transition metal catalysts for C—H functionalization including oxygenation,[3] borylation,[21–24] carbonylation,[25] and dehydrogenation.[26] Ir,[27,28] Rh,[29–31] Re,[32] and Ru[33,34] based catalysts have been extensively used for C—H borylation of hydrocarbon using bis(pinacolato)diboron (B_2Pin_2) as the borylating agent. These studies have emphasized that transition metal-catalyzed C—H borylation of aromatic compounds is an effective, efficient, and reliable strategy for the synthesis of organoboron compounds. Under mild conditions, Ir complexes incorporating bipyridine-based organic linkers exhibited excellent catalytic performances as compared with other transition metal-based catalysts.[35,36] To address the drawbacks of homogeneous catalytic systems such as their lack of recyclability and reusability and the involvement of expensive metals, extraordinary effort has been made by researchers in recent years, and this has led to the development of Ir-based heterogeneous catalysts for C—H borylation.[37] Numerous

heterogeneous platforms including mesoporous silica,[38,39] metal-organic frameworks (MOFs),[40–42] organosilica-nanotubes,[43] and covalent triazine frameworks[44–47] have been reported. These well-established Ir-based materials exhibit high catalytic activity and selectivity for C—H borylation of arenes. However, covalent organic frameworks (COFs) are largely unexploited as decorating platforms for C—H borylation of electronically and sterically substituted arenes.

COFs are porous crystalline polymers with structural periodicity and are composed of organic building blocks linked via covalent bonds.[48–60] Owing to their crystallinity, tunable pore size, high surface area, and chemical and thermal stabilities, COFs can be used in various applications such as catalysis,[61–71] optoelectronic devices,[72–74] environmental remediation,[75–77] energy storage,[78,79] sensors,[80] drug delivery,[81,82] and gas storage and separation.[83–88] COFs have drawn significant attention as heterogeneous catalysts because of their remarkable characteristics such as the high catalytic efficiency and good reusability. The most common strategy to incorporate catalytically active metals or innumerable organic functionalities into COFs is via postsynthetic modifications. For instance, Gao and co-workers reported the bimetallic docking for cascade and tandem reactions.[89,90] Furthermore, Wang *et al.* reported the immobilization of Pd into COF-LZU1 to catalyze the Suzuki-Miyaura coupling reaction,[68] while our group reported the concerted combination of two reactive centers for the conversion of carbon dioxide to value added chemicals.[69] In addition, a *de novo* strategy was employed to construct COFs with catalytic building blocks. For example, Yaghi *et al.* employed a porphyrin monomer to construct porphyrin-based COFs for the electrocatalytic CO_2 reduction,[64] and Cui's group synthesized BINOL-based COFs to catalyze the asymmetric addition reaction of diethylzinc to aldehydes.[91] In addition, Banerjee *et al.* reported that β-ketoenamine linked COFs and porphyrin embellish frameworks were effective organocatalysts for cascade reactions.[92–94] Marinescu and co-workers reported Re(I) bipyridine scaffold to synthesize COFs for CO_2 reduction,[95,96] while our group, in collaboration with Chen and Zhang's research group, recently reported the use of squaramide-decorated COF for organocatalysis.[97] Herein, we demonstrate the immobilization of an Ir-complex on a bipyridine-based COF, Ir_{cod}(I)@Py-2,2′-BPyPh COF, which is a promising and efficacious heterogeneous catalyst for C—H borylation with excellent recyclability, reusability, and retention of crystallinity.

II. EXPERIMENTAL DETAILS

All the reagents and solvents were purchased from commercial sources and used as received without any further purification. Pyrene (Acros Organics, ≥97.5%), 4-(4,4,5,5-tetramethyl-1,3,4-dioxaborolan-2-yl)aniline (Oakwood products, 98%), palladium tetrakis(triphenylphosphine) (Sigma-Aldrich, 99%), potassium carbonate (Sigma-Aldrich, 99%), 5,5′-dimethyl-2,2′-bipyridine (Alfa Aesar, 98%), hexamethylenetetramine (Acros Organics, 99%), bis(pinacolato)diboron (B_2Pin_2) (Oakwood Chemical), hydrochloric acid (Sigma-Aldrich, ACS grade), chloroform (Fischer chemical), dichloromethane (Sigma-Aldrich, ≥99.8%), and tetrahydrofuran (THF) (Acros Organics, 99%) were used as received. 4,4′,4″,4‴-(Pyrene-1,3,6,8-tetrayl)tetraaniline (PyTTA)[98] and 2,2′-bipyridyl-5,5′-dialdehyde (BPyDCA)[99] were synthesized according to previously reported procedures.

^{1}H nuclear magnetic resonance (NMR) and ^{13}C NMR spectra were acquired on a Varian Inova 400 MHz spectrometer. Chemical shifts (δ) are expressed in parts per million (ppm) and are calibrated using an internal standard (^{1}H NMR: $CDCl_3$: 7.26 ppm, DMSO-d_6: 2.46 ppm; ^{13}C NMR: $CDCl_3$: 77.19 ppm, DMSO-d_6: 39.6 ppm). Powder X-ray diffraction (PXRD) data were collected at room temperature on a Bruker AXS D8 Advance A25 X-ray diffractometer (40 kV, 40 mA) using Cu Kα (λ = 1.5406 Å) radiation in the scanning range of 2°–40°. Fourier-transform infrared (FT-IR) spectra were recorded from 4000 cm^{-1} to 400 cm^{-1} using the Perkin Elmer spectrometer with a resolution of 4 cm^{-1}. Thermal gravimetric analysis (TGA) curves were recorded from room temperature to 800 °C at a rate of 10 °C/min using TGA Q50. N_2 adsorption isotherms at 77 K were collected using the Micromeritics ASAP 2020 surface area analyzer, and CO_2 adsorption isotherms were recorded at 298 K using a water bath. The Brunauer-Emmett-Teller (BET) method was used to calculate the specific surface area. The pore volume was derived from the sorption curve by using the nonlocal density functional theory (NLDFT) model. Scanning electron microscopy (SEM) images were collected using a Hitachi S 800 scanning electron microscope. X-ray photoelectron spectroscopic (XPS) analyses were acquired on a Perklin-Elmer PHI 5100 system equipped with a Mg or Al nonmonochromatic, and the binding energies were calibrated using the C 1s peak at 284.8 eV. ^{13}C (100.5 MHz) cross polarization magic-angle spinning (CP-MAS) solid state NMR experiments were performed on a Varian infinity plus 400 spectrometers equipped with a magic-angle spin probe in a 4 mm ZrO_2 rotor. Elemental analyses were performed via flask combustion followed by ion chromatography.

For the electron paramagnetic resonance (EPR) measurement, "Approximately 20 μl of powder was loaded into a borosilicate capillary tube (0.70 mm i.d./1.25 mm o.d.; VitroGlass, Inc.), which was mounted on a Varian E109 spectrometer fitted with a cavity resonator. The continuous wave (CW) EPR spectrum was obtained with an observe power of 12.5 mW and a modulation amplitude of 10 G. The sample was scanned over 200 G, from 3300 G to 3500 G, with an averaging time of ~20 min."

A. Synthesis of Py-2,2′-BPyPh COF

Py-2,2′-BPyPh COF was prepared using a previously reported procedure.[100] A Pyrex tube with o.d. × i.d. = 9.5 mm × 7.5 mm was charged with 2,2′-bipyridyl-5,5′-dialdehyde (8.5 mg, 0.04 mmol) and 4,4′,4″,4‴-(pyrene-1,3,6,8-tetrayl)tetraaniline (11.3 mg, 0.02 mmol) in 1.2 ml of a 5:5:2 (v:v) solution of *o*-dichlorobenzene/*n*-butanol/3M aqueous acetic acid. The tube was flash frozen at 77 K (liquid N_2 bath), evacuated, and flame-sealed. The reaction mixture was heated at 120 °C for 72 h to afford a dark red precipitate which was isolated by filtration and washed with dry tetrahydrofuran and dry acetone. The fluffy powder was dried at 120 °C under vacuum for 24 h.

B. Synthesis of Ir_{cod}(I)@Py-2,2′-BPyPh COF

The reaction was conducted in a Schlenk tube under N_2 atmosphere inside a glove box. In the 50 ml Schlenk tube, as-synthesized

TABLE I. Effect of various catalysts and reaction conditions for preliminary C—H borylation reaction. Reaction conditions: Ir_{cod}(I)@Py-2,2-BPyPh COF (0.6 mol. %, 0.008 mmol of iridium); arene:B_2Pin_2 (substrate to boron reagent molar ratio), 3 ml heptane. Yield was determined by ^{1}H-NMR.

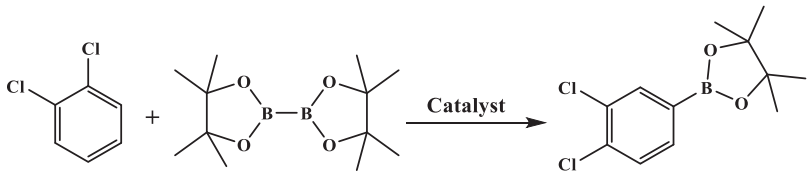

Entry	DCB:B_2Pin_2	Solvent	Temp (°C)	Catalyst	Yield (%)
1	1:0.5	THF	67	Ir_{cod}(I)@Py-2,2′-BPyPh COF	<5
2	1:0.5	DMF	40	Ir_{cod}(I)@Py-2,2′-BPyPh COF	<5
3	1:0.5	Heptane	90	Ir_{cod}(I)@Py-2,2′-BPyPh COF	66
4	1:1	Heptane	90	Ir_{cod}(I)@Py-2,2′-BPyPh COF	87
5	1:1	Heptane	90	[Ir(OMe)(cod)$_2$] + Py-2,2′-BPyPh COF	13
6	1:1	Heptane	90	[Ir(OMe)(cod)$_2$]	<5
7	1:1	Heptane	90	Py-2,2′-BPyPh COF	0

Py-2,2′-BPyPh COF (50 mg) was added into a solution of Ir complex (75 mg) in dry solvent (25 ml). The reaction mixture was stirred at room temperature for 24 h under an inert atmosphere. The resulting precipitate was filtered and washed with anhydrous benzene and anhydrous tetrahydrofuran to remove any unbound metal ions. The product was dried overnight under vacuum before further characterization.

C. Catalytic tests

The catalysis was carried out under inert condition in a 10 ml Schlenk tube on a magnetic stirrer. Typically, B_2Pin_2 (0.125 mmol), an arene (0.125 mmol), 3 ml dry heptane, and catalysts listed in Table I were stirred at elevated temperature for 48 h. After the reactions, the catalysts were washed with excess dry heptane and dry THF and reused for the next catalytic reactions.

D. Recyclability

The catalyst separated after the catalytic reaction was washed with anhydrous solvents and dried overnight at 80 °C. This catalyst was reused for the next catalytic reaction under the same reaction condition. This procedure was repeated multiple times to examine the recyclability of the Ir-immobilized framework.

III. RESULTS AND DISCUSSION

To carry out the C—H borylation, we chose the yellow-colored, two-dimensional, imine linked Py-2,2′-BPyPh COF containing bipyridine functionalities, which was fabricated via the condensation reaction of 4,4′,4″,4‴-(pyrene-1,3,6,8-tetrayl)tetraaniline (PyTTA) and 2,2′-bipyridyl-5,5′-dialdehyde (BPyDCA) in the presence of 3M acetic acid according to the literature.[100] Clear diffraction peaks at 3.2°, 4.6°, 6.4°, 9.8°, 12.9°, and 23.9°, corresponding to the (110), (020), (220), (330), (440), and (001) facets, respectively, suggest that Py-2,2′-BPyPh COF was highly crystalline (Fig. S2). The disappearance of —C=O band at 1624 cm^{-1} in FT-IR spectrum and emergence of a peak corresponding to —C=N at 159.8 ppm in the ^{13}C CP-MAS NMR spectrum confirmed the chemical composition of the framework (Figs. S3 and S4). The surface area measurement revealed that the BET and Langmuir surface area were 1785 m^2 g^1 and 2746 m^2 g^{-1}, respectively, while the pore size was 2.3 nm. The TGA curves suggested that the synthesized material possessed high thermal stability up to 450 °C. This indicates that the COF has substantial potential as a decorating platform for borylation reactions (Figs. S5–S8).

Inspired by the essential characteristics such as uniform distribution of bipyridine moieties associated with Py-2,2′-BPyPh COF and in-depth chemistry of Ir-catalyzed C—H borylation, we synthesized Ir_{cod}(I)@Py-2,2′-BPyPh COF by the reaction of Py-2,2′-BPyPh COF and [Ir(OMe)(1,5-cod)]$_2$ under inert condition [Fig. 1(a)]. Once Ir was immobilized, the color of the framework changed to dark brown; 3.1 wt. % Ir was incorporated in Ir_{cod}(I)@Py-2,2′-BPyPh COF as analyzed by inductively coupled mass spectrometry. SEM images showed no change in morphology of Ir_{cod}(I)@Py-2,2′-BPyPh COF. A uniform distribution of Ir was observed by energy dispersive X-ray spectroscopy mapping via SEM (Fig. S9), indicating that Ir decoration ensues completely within the immobilized crystalline framework. In order to further understand the docking status of Ir, we performed X-ray photoelectron spectroscopy (XPS), ^{13}C MAS NMR spectroscopy, and electron paramagnetic resonance (EPR) spectroscopy. The XPS spectrum of Ir_{cod}(I)@Py-2,2′-BPyPh COF displayed binding energies of Ir $4f_{5/2}$ and Ir $4f_{7/2}$ at 64.8 eV and 61.9 eV, respectively [Fig. 2(a)]. In addition, the N 1s peak was blue shifted to 399.5 eV as compared with that in pristine Py-2,2′-BPyPh COF (398.1 eV) [Figs. 2(b) and 2(c)].

The ^{13}C MAS NMR spectra of Ir_{cod}(I)@Py-2,2′-BPyPh COF showed peaks corresponding to cyclooctadiene and methoxy peaks at 99.84, 39.21, and 28.71 ppm (Fig. S10), without any variation in the chemical shift of the imine functionalities at 156.6 ppm. Similar observations have been reported for Ir immobilization on

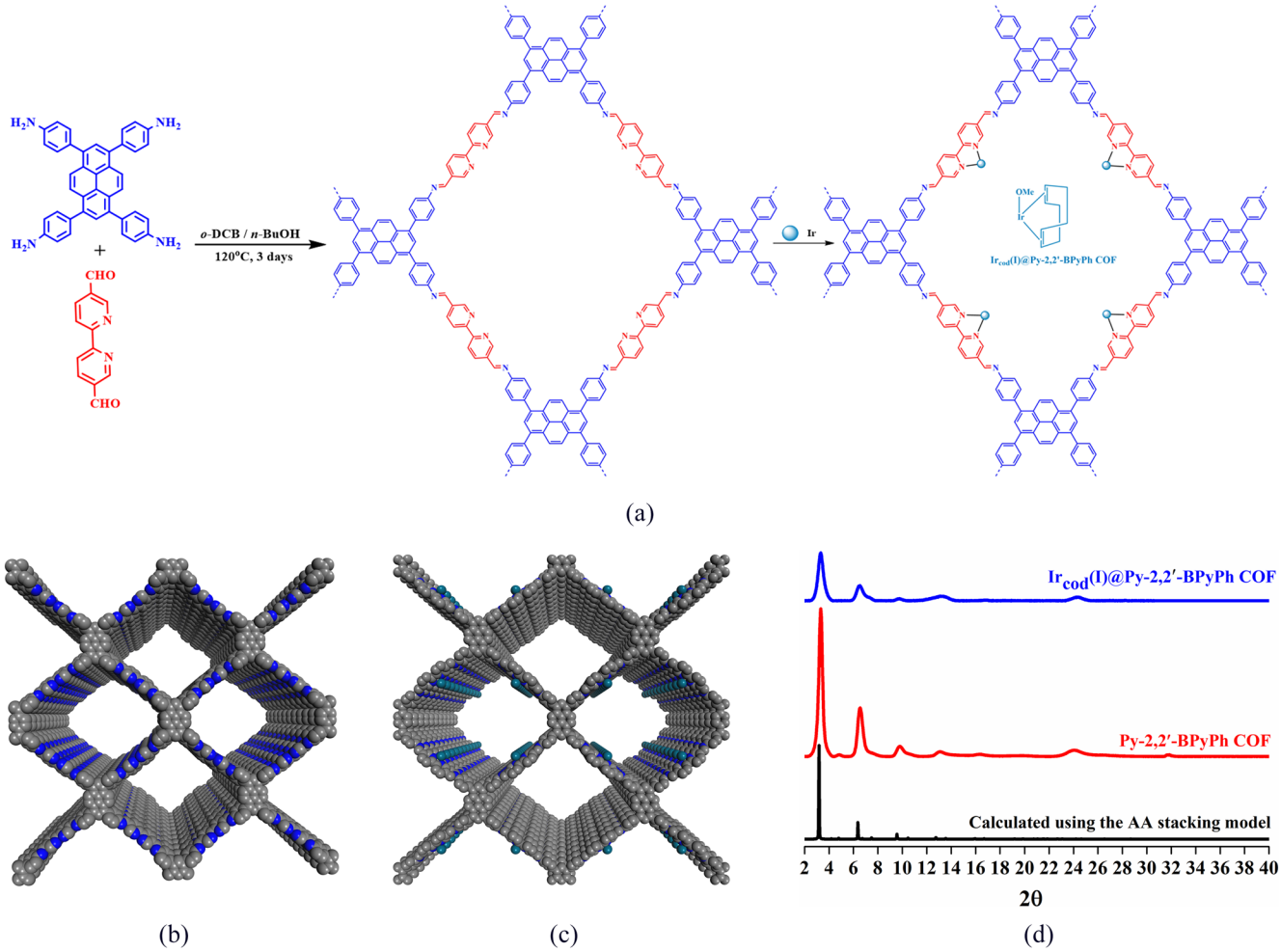

FIG. 1. (a) Schematic representation of 2D Py-2,2′-BPyPh COF and Ir$_{cod}$(I)@Py-2,2′-BPyPh COF synthesis. Graphic extended view of the stacking structure (b) Py-2,2′-BPyPh COF and (c) Ir$_{cod}$(I)@Py-2,2′-BPyPh COF. (d) Comparison of experimental and calculated PXRD pattern of Py-2,2′-BPyPh COF and Ir$_{cod}$(I)@Py-2,2′-BPyPh COF.

mesoporous silica as a heterogeneous support.[43,101] EPR spectroscopy was performed to evaluate the electronic structure of the Ir complex decorated on the framework. The spectrum [Fig. 2(d)] is consistent with the expected electronic environment and oxidation state. Similar characteristics were also observed by Braunstein and co-workers for iridium (I) complexes.[102] All these results obtained using various spectroscopic techniques suggest the existence of strong interactions between Ir and the bipyridine functionalities in Ir$_{cod}$(I)@Py-2,2′-BPyPh COF.

PXRD patterns validate that the crystalline nature of Py-2,2′-BPyPh COF is preserved during Ir immobilization. However, the resultant peaks are broad, and the relative intensity of the (110) facet decreases in Ir$_{cod}$(I)@Py-2,2′-BPyPh COF during the postsynthetic modification [Fig. 1(d)]. This is apparently because of the incorporation of Ir functionalities; a similar retention of the structure during various chemical modifications or modifications with metals has been observed for COFs.[68–71,89,90] The peak at 1625 cm^{-1} in the FT-IR spectrum of Ir$_{cod}$(I)@Py-2,2′-BPyPh COF further confirmed the retention of the imine functionalities during docking (Fig. S11). To examine the porosity of Ir$_{cod}$(I)@Py-2,2′-BPyPh COF, N_2 sorption measurements were performed at 77 K. As expected, a substantial decrease in the BET surface area and pore size (nonlocal density functional theory) was observed. The BET surface area and the pore size decreased from 1785 m^2 g^{-1} to 2.3 nm for pristine Py-2,2′-BPyPh COF to 859 m^2 g^{-1} and 1.59 nm, respectively, for Ir$_{cod}$(I)@Py-2,2′-BPyPh COF (Fig. 3). Although the pores of the immobilized framework were partially bound by active Ir metal, the surface area and the open structure were still significant for imparting catalytic activity within the pore channel. The good thermal stability (>215 °C) of Ir$_{cod}$(I)@Py-2,2′-BPyPh COF (Fig. S13) as confirmed by TGA prompted us to employ Ir-immobilized framework for C—H borylation at an elevated temperature.

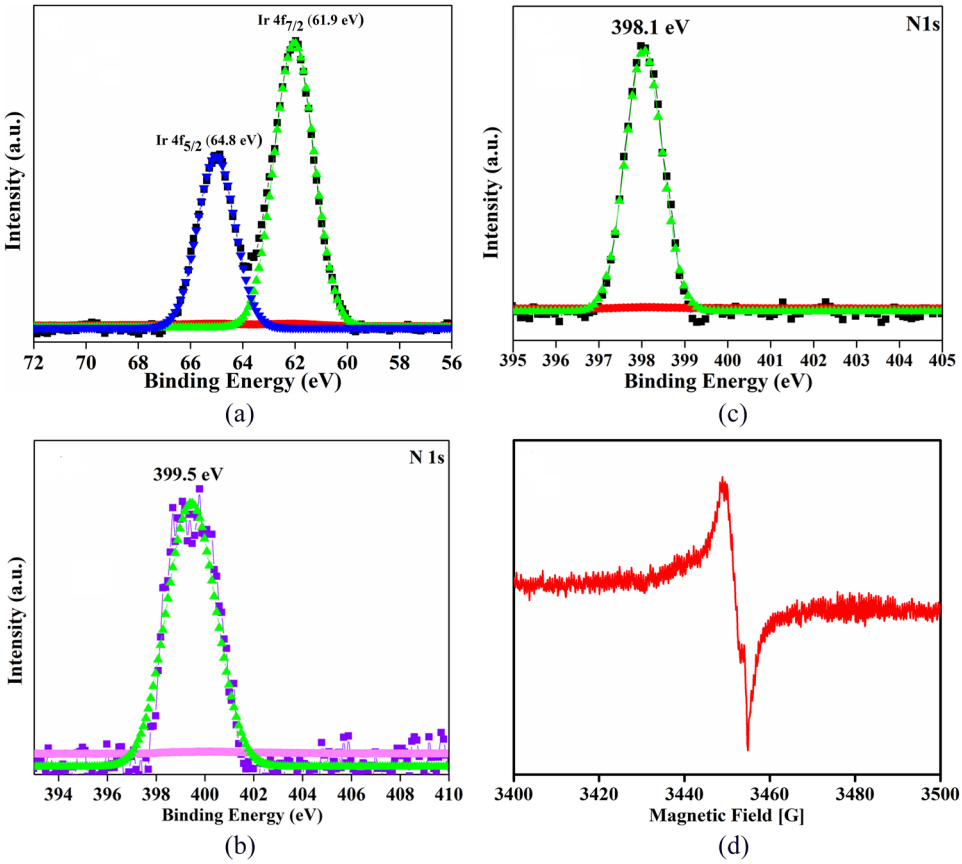

FIG. 2. XPS Spectra of (a) $Ir_{cod}(I)$@Py-2,2′-BPyPh COF (iridium); (b) $Ir_{cod}(I)$@Py-2,2′-BPyPh COF (nitrogen); (c) Py-2,2′-BPyPh COF (nitrogen); and (d) EPR spectra of $Ir_{cod}(I)$@Py-2,2′-BPyPh COF.

Given the role of Ir chemistry in C−H activation and the successful immobilization of Ir in the pore channels of 2D bipyridine functionalized Py-2,2′-BPyPh framework, we attempted to evaluate the performance of $Ir_{cod}(I)$@Py-2,2′-BPyPh COF in C−H borylation reactions. Before optimizing the reaction condition, we investigated the stability of the immobilized framework in protic and aprotic solvent by PXRD and FT-IR spectroscopy (Figs. S14 and S15). Initially, the arene, 1,2-dichlorobenzene, was reacted in the presence of B_2Pin_2 in various solvents at an elevated temperature using the Ir docked framework as a catalyst.

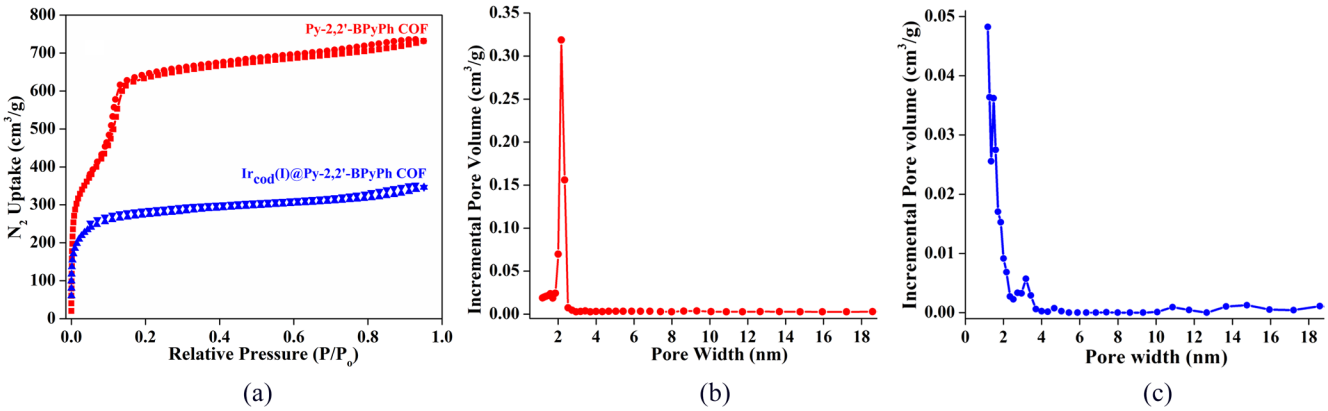

FIG. 3. N_2 sorption isotherms comparison of (a) Py-2,2′-BPyPh COF and $Ir_{cod}(I)$@Py-2,2′-BPyPh COF; pore size distribution curve from N_2 adsorption data of (b) Py-2,2′-BPyPh COF and (c) $Ir_{cod}(I)$@Py-2,2′-BPyPh COF.

Almost no borylated products were obtained in polar solvents such as tetrahydrofuran, dichloromethane, and dimethylformamide. However, in nonpolar solvent such as heptane, borylated products with appropriate stoichiometric ratios were obtained in 66% and 87% yields (Table I, Entry 3 and 4). These results are summarized in Table I and are in agreement with previously reported studies on the role of solvents and temperature.[39,103] In addition, a set of control experiments were conducted to demonstrate the catalytic properties of the Ir immobilized framework. Apparently, poor catalytic activity was observed for the borylation of 1,2-dichlorobenzene using [Ir(OMe)(cod)$_2$], Py-2,2′-BPyPh COF, [Ir(OMe)(cod)$_2$] + Py-2,2′-BPyPh COF under the

TABLE II. Ir$_{cod}$(I)@Py-2,2′-BPyPh COF catalyzed C—H borylation of arenes and heteroarenes. Reaction conditions: Ir$_{cod}$(I)@Py-2,2-BPyPh COF (0.008 mmol of iridium, 0.6 mol. %); arene (0.125 mmol); B_2Pin_2 (0.125 mmol), and heptane (3 ml).

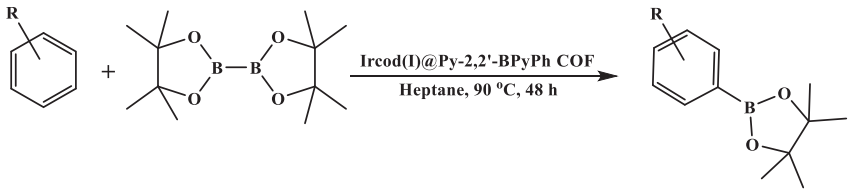

Entry	Substrate	Product	Yield (%)
1	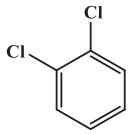	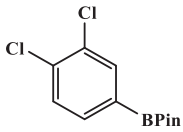	87
2	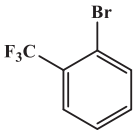	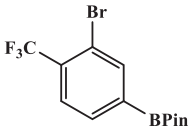	71
3	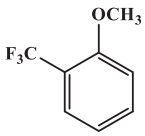	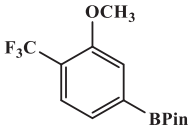	42
4	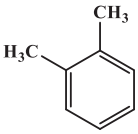	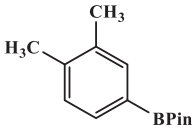	49
5	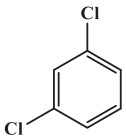	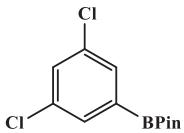	81
6	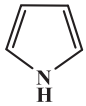	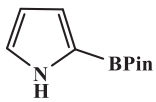	67
7		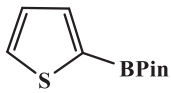	62

optimized reaction conditions (Table I, Entry 5–7). Furthermore, an appropriate stoichiometric ratio of arene and B_2Pin_2 is necessary to obtain substantial catalytic conversion. Notably, the Ir_{cod}(I)@Py-2,2′-BPyPh COF heterogeneous catalyst exhibited a sluggish initial reactivity as evident from the kinetic profile of the catalyst (Fig. S16). We performed a hot filtration test to demonstrate the heterogeneity of the catalytic process. After filtering the catalyst, the catalyst-free solution was subjected overnight to similar reaction condition. No catalytic activity was observed for C—H borylation reaction in the absence of the catalyst, thereby confirming the heterogeneity of Ir_{cod}(I)@Py-2,2′-BPyPh COF.

After assessing the catalytic activity, optimum reaction conditions, and heterogeneity of Ir_{cod}(I)@Py-2,2′-BPyPh COF, we further studied the substrate scope for various arenes and heteroarenes featuring electron-withdrawing and electron-donating substituents in C—H borylation. Table II shows that Ir_{cod}(I)@Py-2,2′-BPyPh COF catalyzes a range of substrates, giving moderate to excellent yields of the borylated products. Specifically, the electron-withdrawing substituents afford excellent conversion, while the electron-donating substituents afforded moderate conversion. For instance, 3-bromobenzotrifluoride and 3-(trifluoromethyl)anisole afforded 71% and 42% conversion, respectively. Moreover, the borylation reactivity of the heteroarenes was predominantly influence by electronic effects, i.e., the presence of C—H bond in the α position with respect to the heteroatom (Entry 6 and 7). Hartwig and Miyaura proposed the mechanism of C—H borylation highlighting three core steps:[23,104] oxidative addition, reductive elimination, and regeneration of catalyst (Fig. S17). During the catalytic conversion, Ir(I) is converted to Ir(III) upon treatment with B_2pin_2. This is followed by the oxidative addition to arene/substituted arene to form an Ir(V) species. Ir(V) undergoes reductive elimination to form Ir(III) and organoboron compounds, along with regeneration of the Ir catalyst. It was also observed that varying the arene to B_2pin_2 molar ratio from 1:0.5 to 1:1 and mol. % of Ir_{cod}(I)@Py-2,2′-BPyPh framework increased the percentage yield. This was consistent with the kinetics observed by other research group to establish the mechanistic pathway.[105,106] The core significance of heterogeneity lies in reusability, recyclability, and feasibility in industrial application. The Ir catalyst was recovered by centrifugation, washed, and dry under vacuum and employed for the next catalytic reaction. The percentage yield of the 1,2-dichlorobenzene borylation product up to four successive runs was around 75%, thereby indicates good recyclability (Fig. 4) of the catalyst. The well-preserved PXRD pattern, FT-IR spectrum, and SEM physiochemical analysis after the catalysis verified the stability of the Ir docked framework in terms of retention of crystallinity, imine functionalities, and morphology (Figs. S18–S20). We further compared the surface areas and EPR spectra of the pristine and recycled Ir_{cod}(I)@Py-2,2′-BPyPh COF. No changes in electronic and oxidation environment occurred as evident from the EPR spectra; however, the BET surface area decreased slightly from 859 $m^2\ g^{-1}$ to 739 $m^2\ g^{-1}$ (Figs. S21 and S22). The entire analyses suggested good stability of the synthesized catalyst, which could be reused up to four catalytic cycles while preserving its crystallinity. The importance of Ir immobilization on COF as a decorating platform for pivotal C—H borylation reactions is also realized.

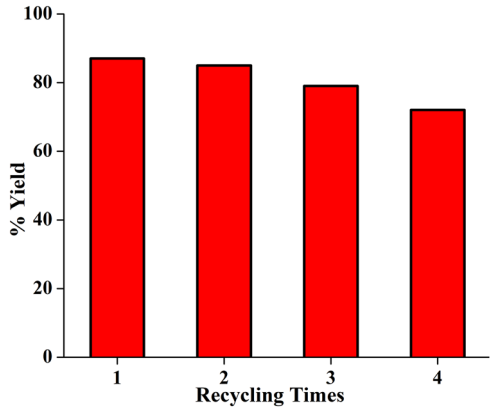

FIG. 4. Reusability test of Ir_{cod}(I)@Py-2,2′-BPyPh COF catalyst for C—H borylation.

IV. CONCLUSION

In summary, we have developed a programmed synthetic procedure for the immobilization of Ir on bipyridine functionalized COFs. The Ir(I)-immobilized framework was highly porous, had good thermal stability, and retained its crystallinity after post-synthetic modification. Furthermore, Ir_{cod}(I)@Py-2,2′-BPyPh COF demonstrated excellent catalytic performance for a range of electronically and sterically substituted substrates for C—H borylation. In contrast to its homogeneous counterpart, this heterogeneous catalyst can be easily recycled and reused. Our strategy paves way for the immobilization of transition metal-based catalysts into COFs via pore surface engineering, thereby broadening the scope of heterogeneous catalysis and other highly valued applications.

SUPPLEMENTARY MATERIAL

See supplementary material for the complete synthetic procedures and characterizations of Ir_{cod}(I)@Py-2,2′-BPyPh COF.

ACKNOWLEDGMENTS

The authors acknowledge the University of South Florida (USF) for support of this work. We also extend our sincere appreciation to the Deanship of Scientific Research at King Saud University (KSU) for funding this project through Research Group (RG No. 236) and RSSU for their technical support. X-ray photoelectron spectroscopy studies were carried in the Nebraska Nanoscale Facility, Nebraska Center for Materials and Nanoscience, which is supported by the NSF under award NNCI Grant No. 1542182, and the Nebraska Research Initiative (NRI).

REFERENCES

[1] J.-Q. Yu and Z.-J. Shi, *C-H Activation: Topics in Current Chemistry* (Springer, Berlin, 2010), Vol. 292.
[2] R. H. Crabtree, Chem. Rev. **85**, 245 (1985).
[3] A. E. Shilov and G. B. Shul'pin, Chem. Rev. **97**, 2879 (1997).
[4] G. Dyker, Angew. Chem., Int. Ed. **38**, 1698 (1999).
[5] J. H. Lunsford, Catal. Today **63**, 165 (2000).
[6] R. H. Crabtree, J. Organomet. Chem. **689**, 4083 (2004).
[7] J. F. Hartwig, Nature **455**, 314 (2008).
[8] D. A. Colby, R. G. Bergman, and J. A. Ellman, Chem. Rev. **110**, 624 (2010).

[9]D. Balcells, E. Clot, and O. Eisenstein, Chem. Rev. **110**, 749 (2010).
[10]T. Newhouse and P. S. Baran, Angew. Chem., Int. Ed. **50**, 3362 (2011).
[11]R. B. Bedford, S. J. Durrant, and M. Montgomery, Angew. Chem., Int. Ed. **127**, 8911 (2015).
[12]J. A. Labinger, Chem. Rev. **117**, 8483 (2017).
[13]P. Schwach, X. Pan, and X. Bao, Chem. Rev. **117**, 8497 (2017).
[14]R. Shang, L. Ilies, and E. Nakamura, Chem. Rev. **117**, 9086 (2017).
[15]J. F. Hartwig, Acc. Chem. Res. **50**, 549 (2017).
[16]Y. Qin, L. Zhu, and S. Luo, Chem. Rev. **117**, 9433 (2017).
[17]R. H. Crabtree and A. Lei, Chem. Rev. **117**, 8481 (2017).
[18]D. J. Abrams, P. A. Provencher, and E. J. Sorensen, Chem. Soc. Rev. **47**, 8925 (2018).
[19]D. Kang, K. Ahn, and S. Hong, Asian J. Org. Chem. **7**, 1136 (2018).
[20]P. Gandeepan, T. Müller, D. Zell, G. Cera, S. Warratz, and L. Ackermann, Chem. Rev. **119**, 2192 (2019).
[21]T. Ishiyama and N. Miyaura, J. Organomet. Chem. **680**, 3 (2003).
[22]J. F. Hartwig, Chem. Soc. Rev. **40**, 1992 (2011).
[23]I. A. I. Mkhalid, J. H. Barnard, T. B. Marder, J. M. Murphy, and J. F. Hartwig, Chem. Rev. **110**, 890 (2010).
[24]J. F. Hartwig, Acc. Chem. Res. **45**, 864 (2012).
[25]T. Sakakura, T. Sodeyama, K. Sasaki, K. Wada, and M. Tanaka, J. Am. Chem. Soc. **112**, 7221 (1990).
[26]J. Choi, A. H. R. MacArthur, M. Brookhart, and A. S. Goldman, Chem. Rev. **111**, 1761 (2011).
[27]C. W. Liskey and J. F. Hartwig, J. Am. Chem. Soc. **134**, 12422 (2012).
[28]C. W. Liskey and J. F. Hartwig, J. Am. Chem. Soc. **135**, 3375 (2013).
[29]H. Chen, S. Schlecht, T. C. Semple, and J. F. Hartwig, Science **287**, 1995 (2000).
[30]C. S. Wei, C. A. Jiménez-Hoyos, M. F. Videa, J. F. Hartwig, and M. B. Hall, J. Am. Chem. Soc. **132**, 3078 (2010).
[31]J. F. Hartwig, K. S. Cook, M. Hapke, C. D. Incarvito, Y. Fan, C. E. Webster, and M. B. Hall, J. Am. Chem. Soc. **127**, 2538 (2005).
[32]H. Chen and J. F. Hartwig, Angew. Chem., Int. Ed. **38**, 3391 (1999).
[33]J. M. Murphy, J. D. Lawrence, K. Kawamura, C. Incarvito, and J. F. Hartwig, J. Am. Chem. Soc. **128**, 13684 (2006).
[34]A. K. Cook, S. D. Schimler, A. J. Matzger, and M. S. Sanford, Science **351**, 1421 (2016).
[35]E. Fernández and A. M. Segarra, *Iridium Complexes in Organic Synthesis* (Wiley-VCH Verlag GmbH and Co. KGaA, 2009), p. 173.
[36]T. Ishiyama, J. Takagi, K. Ishida, N. Miyaura, N. R. Anastasi, and J. F. Hartwig, J. Am. Chem. Soc. **124**, 390 (2002).
[37]S. Santoro, S. I. Kozhushkov, L. Ackermann, and L. Vaccaro, Green Chem. **18**, 3471 (2016).
[38]S. Kawamorita, H. Ohmiya, K. Hara, A. Fukuoka, and M. Sawamura, J. Am. Chem. Soc. **131**, 5058 (2009).
[39]F. Wu, Y. Feng, and C. W. Jones, ACS Catal. **4**, 1365 (2014).
[40]K. Manna, T. Zhang, and W. Lin, J. Am. Chem. Soc. **136**, 6566 (2014).
[41]M. I. Gonzalez, E. D. Bloch, J. A. Mason, S. J. Teat, and J. R. Long, Inorg. Chem. **54**, 2995 (2015).
[42]K. Manna, T. Zhang, F. X. Greene, and W. Lin, J. Am. Chem. Soc. **137**, 2665 (2015).
[43]S. Zhang, H. Wang, M. Li, J. Han, X. Liu, and J. Gong, Chem. Sci. **8**, 4489 (2017).
[44]N. Tahir, F. Muniz-Miranda, J. Everaert, P. Tack, T. Heugebaert, K. Leus, L. Vincze, C. V. Stevens, V. Van Speybroeck, and P. Van Der Voort, J. Catal. **371**, 135 (2019).
[45]G. H. Gunasekar, K. Park, V. Ganesan, K. Lee, N.-K. Kim, K.-D. Jung, and S. Yoon, Chem. Mater. **29**, 6740 (2017).
[46]E. Rozhko, M. G. Goesten, T. Wezendonk, B. Seoane, F. Kapteijn, M. Makkee, and J. Gascon, ChemCatChem **8**, 2217 (2016).
[47]M. Liu, L. Guo, S. Jin, and B. Tan, J. Mater. Chem. A. **7**, 5153 (2019).
[48]N. Huang, P. Wang, and D. Jiang, Nat. Rev. Mater. **1**, 16068 (2016).
[49]C. S. Diercks and O. M. Yaghi, Science **355**, eaal1585 (2017).
[50]Y. Jin, Y. Hu, and W. Zhang, Nat. Rev. Chem. **1**, 0056 (2017).
[51]A. P. Côté, A. I. Benin, N. W. Ockwig, M. O'Keeffe, A. J. Matzger, and O. M. Yaghi, Science **310**, 1166 (2005).
[52]X. Feng, X. Ding, and D. Jiang, Chem. Soc. Rev. **41**, 6010 (2012).
[53]S.-Y. Ding and W. Wang, Chem. Soc. Rev. **42**, 548 (2013).
[54]R. P. Bisbey and W. R. Dichtel, ACS Cent. Sci. **3**, 533 (2017).
[55]F. Beuerle and B. Gole, Angew. Chem., Int. Ed. **57**, 4850 (2018).
[56]Y. Song, Q. Sun, B. Aguila, and S. Ma, Adv. Sci. **6**, 1801410 (2019).
[57]S. Kandambeth, K. Dey, and R. Banerjee, J. Am. Chem. Soc. **141**, 1807 (2019).
[58]P. J. Waller, F. Gandara, and O. M. Yaghi, Acc. Chem. Res. **48**, 3053 (2015).
[59]M. S. Lohse and T. Bein, Adv. Funct. Mater. **28**, 1705553 (2018).
[60]T. Ma, E. A. Kapustin, S. X. Yin, L. Liang, Z. Zhou, J. Niu, H. Li, Y. Wang, J. Su, J. Li, X. Wang, W. D. Wang, W. Wang, J. Sun, and O. M. Yaghi, Science **361**, 48 (2018).
[61]J. Zhang, X. Han, X. Wu, Y. Liu, and Y. Cui, J. Am. Chem. Soc. **139**, 8277 (2017).
[62]Q. Sun, B. Aguila, P. C. Lan, and S. Ma, Adv. Mater. **31**, 1900008 (2019).
[63]Q. Sun, Y. Tang, B. Aguila, S. Wang, F.-S. Xiao, P. K. Thallapally, A. M. Al-Enizi, A. Nafady, and S. Ma, Angew Chem., Int. Ed. **58**, 8670 (2019).
[64]C. S. Diercks, S. Lin, N. Kornienko, E. A. Kapustin, E. M. Nichols, C. Zhu, Y. Zhao, C. J. Chang, and O. M. Yaghi, J. Am. Chem. Soc. **140**, 1116 (2018).
[65]P.-F. Wei, M.-Z. Qi, Z.-P. Wang, S.-Y. Ding, W. Yu, Q. Liu, L.-K. Wang, H.-Z. Wang, W.-K. An, and W. Wang, J. Am. Chem. Soc. **140**, 4623 (2018).
[66]Q. Sun, C.-W. Fu, B. Aguila, J. A. Perman, S. Wang, H.-Y. Huang, F.-S. Xiao, and S. Ma, J. Am. Chem. Soc. **140**, 984 (2018).
[67]S. Lin, C. S. Diercks, Y.-B. Zhang, M. Kornienko, E. M. Nichols, Y. Zhao, A. R. Paris, D. Kim, P. Yang, O. M. Yaghi, and C. J. Chang, Science **349**, 1208 (2015).
[68]S.-Y. Ding, J. Gao, Q. Wang, Y. Zhang, W.-G. Song, C.-Y. Su, and W. Wang, J. Am. Chem. Soc. **133**, 19816 (2011).
[69]Q. Sun, B. Aguila, J. A. Perman, N. Nguyen, and S. Ma, J. Am. Chem. Soc. **138**, 15790 (2016).
[70]H. Vardhan, G. Verma, S. Ramani, A. Nafady, A. M. Al-Enizi, Y. Pan, Z. Yang, and S. Ma, ACS Appl. Mater. Interfaces **11**, 3070 (2019).
[71]H. Vardhan, L. Hou, E. Yee, A. Nafady, M. A. Al-Abdrabalnabi, A. M. Al-Enizi, Y. Pan, Z. Yang, and S. Ma, ACS Sustainable Chem. Eng. **7**, 4878 (2019).
[72]G. H. V. Bertrand, V. K. Michaelis, T.-C. Ong, R. G. Griffin, and M. Dincă, Proc. Natl. Acad. Sci. U. S. A. **110**, 4923 (2013).
[73]M. Calik, F. Auras, L. M. Salonen, K. Bader, I. Grill, M. Handloser, D. D. Medina, M. Dogru, F. Löbermann, D. Trauner, A. Hartschuh, and T. Bein, J. Am. Chem. Soc. **136**, 17802 (2014).
[74]L. Chen, K. Furukawa, J. Gao, A. Nagai, T. Nakamura, Y. Dong, and D. Jiang, J. Am. Chem. Soc. **136**, 9806 (2014).
[75]Q. Sun, B. Aguila, J. Perman, L. Earl, C. Abney, Y. Cheng, H. Wei, N. Nguyen, L. Wojtas, and S. Ma, J. Am. Chem. Soc. **139**, 2786 (2017).
[76]Q. Sun, B. Aguila, L. D. Earl, C. W. Abney, L. Wojtas, P. K. Thallapally, and S. Ma, Adv. Mater. **30**, 1705479 (2018).
[77]Q. Sun, B. Aguila, J. Perman, T. Butts, F.-S. Xiao, and S. Ma, Chem **4**, 1726 (2018).
[78]C. R. DeBlase, K. E. Silberstein, T. T. Truong, H. D. Abruna, and W. R. Dichtel, J. Am. Chem. Soc. **135**, 16821 (2013).
[79]S. Wang, Q. Wang, P. Shao, Y. Han, X. Gao, L. Ma, S. Yuan, X. Ma, J. Zhou, X. Feng, and B. Wang, J. Am. Chem. Soc. **139**, 4258 (2017).
[80]N. Huang, X. Ding, J. Kim, H. Ihee, and D. Jiang, Angew. Chem., Int. Ed. **127**, 8828 (2015).
[81]Q. Fang, J. Wang, S. Gu, R. B. Kaspar, Z. Zhuang, J. Zheng, H. Guo, S. Qiu, and Y. Yan, J. Am. Chem. Soc. **137**, 8352 (2015).
[82]S. Mitra, H. S. Sasmal, T. Kundu, S. Kandambeth, I. Kavya, D. Díaz, and R. Banerjee, J. Am. Chem. Soc. **139**, 4513 (2017).
[83]Y. Du, H. Yang, J. M. Whiteley, S. Wan, Y. Jin, S.-H. Lee, and W. Zhang, Angew. Chem., Int. Ed. **55**, 1737 (2016).
[84]C. J. Doonan, D. J. Tranchemontagne, T. G. Glover, J. R. Hunt, and O. M. Yaghi, Nat. Chem. **2**, 235 (2010).
[85]Y. Zeng, R. Zou, and Y. Zhao, Adv. Mater. **28**, 2855 (2016).
[86]L. A. Baldwin, J. W. Crowe, D. A. Pyles, and P. L. McGrier, J. Am. Chem. Soc. **138**, 15134 (2016).
[87]Y. Pramudya and J. L. Mendoza-Cortes, J. Am. Chem. Soc. **138**, 15204 (2016).

[88]Y. Yang, M. Faheem, L. Wang, Q. Meng, H. Sha, N. Yang, Y. Yuan, and G. Zhu, ACS Cent. Sci. **4**, 748 (2018).
[89]W. Leng, Y. Peng, J. Zhang, H. Lu, X. Feng, R. Ge, B. Dong, B. Wang, X. Hu, and Y. Gao, Chem. Eur. J. **22**, 9087 (2016).
[90]W. Leng, R. Ge, B. Dong, C. Wang, and Y. Gao, RSC Adv. **6**, 37403 (2016).
[91]X. Wang, X. Han, J. Zhang, X. Wu, Y. Liu, and Y. Cui, J. Am. Chem. Soc. **138**, 12332 (2016).
[92]M. Bhadra, S. Kandambeth, M. K. Sahoo, M. Addicoat, E. Balaraman, and R. Banerjee, J. Am. Chem. Soc. **141**, 6152 (2019).
[93]M. Bhadra, H. S. Sasmal, A. Basu, S. P. Midya, S. Kandambeth, P. Pachfule, E. Balaraman, and R. Banerjee, ACS Appl. Mater. Interfaces **9**, 13785 (2017).
[94]D. B. Shinder, S. Kandambeth, P. Pachfule, R. R. Kumar, and R. Banerjee, Chem. Commun. **51**, 310 (2015).
[95]D. A. Popov, J. M. Luna, N. M. Orchanian, R. Haiges, C. A. Downes, and S. C. Marinescu, Dalton Trans. **47**, 17450 (2018).
[96]E. M. Johnson, R. Haiges, and S. C. Marinescu, ACS Appl. Mater. Interfaces **10**, 37919 (2018).
[97]X. Li, Z. Wang, J. Sun, J. Gao, Y. Zhao, P. Cheng, B. Aguila, S. Ma, Y. Chen, and Z. Zhang, Chem. Commun. **55**, 5423 (2019).
[98]N. Huang, P. Wang, M. A. Addicoat, T. Heine, and D. Jiang, Angew. Chem., Int. Ed. **129**, 5064 (2017).
[99]M. H. Al-Sayah and A. S. Salameh, Arab. J. Sci. Eng. **25**, 67 (2000).
[100]X. Chen, N. Huang, J. Gao, H. Xu, F. Xu, and D. Jiang, Chem. Commun. **50**, 6161 (2014).
[101]Y. Maegawa and S. Inagaki, Dalton Trans. **44**, 13007 (2015).
[102]F. He, L. Ruhlmann, J.-P. Gisselbrecht, S. Choua, M. Orio, M. Wesolek, A. A. Danapoulos, and P. Braunstein, Dalton Trans. **44**, 17030 (2015).
[103]T. Ishiyama, J. Takagi, J. F. Hartwig, and N. Miyaura, Angew. Chem., Int. Ed. **41**, 3056 (2002).
[104]T. M. Boller, J. M. Murphy, M. Hapke, T. Ishiyama, N. Miyaura, and J. F. Hartwig, J. Am. Chem. Soc. **127**, 14263 (2005).
[105]S. M. Preshlock, B. Ghaffari, P. E. Maligres, S. W. Krska, R. E. Maleczka, Jr., and M. R. Smith III, J. Am. Chem. Soc. **135**, 7572 (2013).
[106]M. A. Larsen and J. F. Hartwig, J. Am. Chem. Soc. **136**, 4287 (2014).